

The Influence of Crystallization and Entrainment of
Cooler Material on the Emplacement of
Basaltic Aa Lava Flows

Joy Crisp

Jet Propulsion Laboratory

California Institute of Technology, Pasadena, CA 91109

Stephen Baloga

Proxemy Research, inc.

Laytonsville, MD 20882

ABSTRACT

A theoretical model is used to describe and investigate the effects of simultaneous crystallization, radiation loss, and entrainment of cooler material on the temperature of a well-mixed core of an active aa lava flow. Entrainment of crust, levee debris, and base material into the interior of active flows has been observed, but the degree of assimilation and thermal consequences are difficult to quantify. The rate of entrainment can be constrained by supplementing the theoretical model with information on the crystallization along the path of the flow and estimation of the radiative loss from the flow interior. Application of the model is demonstrated with the 1984 Mauna Loa flow, which was erupted about 30°C undercooled. Without any entrainment of cooler material, the high crystallization rates would have driven temperatures in the core well above temperatures measured by thermocouple and estimated from glass geothermometry. One plausible scenario for this flow, which agrees with available temperature and crystallinity measurements, has a high initial rate of entrainment during the first 8 hours of travel (a mass ratio of entrained material to fluid core of about 15% if the average temperature of the entrained material was 600°C), which counterbalances the latent heat from approximately 40% crystallization; in this scenario, the model suggests an additional 5% crystallization and a 5% entrainment mass ratio over the subsequent 16-hour period. Measurements of crystallization, radiative losses, and entrainment factors are necessary for understanding the detailed thermal histories of active lava flows.

INTRODUCTION

Cooling and crystallization of the interior of an active basaltic aa lava flow are two important factors that can halt flow advance [e.g., *Guest et al.*, 1987]. Lavas reach a critical viscosity at

about 60% crystal linity, beyond which flow advance ceases [e. g., *Marsh, 1981; Metzner, 1985; Ryerson et al., 1988; Pinkerton and Stevenson, 1992*]. When crystal loading stagnates the advance of a flow front, it can induce breakouts upstream and thus control the final length of the plugged channel and the final arrangement of flows in a composite field [e.g., *Wadge, 1978; Kilburn and Lopes, 1991*]. A predictive model for the cooling of the core as a function of time or distance from the vent provides a means for constraining eruption duration, flow velocities, and eruption rates for unwitnessed terrestrial and planetary lava flows [*Crisp and Baloga, 1990*]. This approach is also useful for evaluating the influence of physical processes on core cooling for different eruption conditions and different values of the parameters in the model.

Numerous models have investigated the cooling of lava flows by radiation from the upper surface of the flow and by conduction of heat into the crust or underlying flow bed [e.g., Gratz number formulations, *Pinkerton and Sparks, 1976; Hulme and Fielder, 1977; Guest et al., 1987; Wilson and Parfitt, 1993*]. However, the thermal history of a flow can be complicated by the release of latent heat from crystallization. For a basalt, the latent heat release can be as high as $(1.75 \text{ to } 2.25) \times 10^6$ Joules per kilogram of lava for 60% crystallization [*Peck et al., 1977; Settle, 1979*], and this can have a strong influence on the heat budget and nature of emplacement of an active flow [*Harrison and Rooth, 1976; Settle, 1979; Crisp and Baloga, 1991; Crisp et al., 1993; Stasiuk et al., 1993*]. The amount of crystals that form while a flow is actively advancing depends on magma composition, eruption temperature, intensity of mixing agitation [*Emerson, 1926; Jaggar, 1930; Macdonald, 1953; Kouchi et al., 1986*], and the temperature and degassing history [*Sparks and Pinkerton, 1978*]. Other than *Crisp et al. [1993]*, the amount of crystallization that occurs during the emplacement of lava flows has not been documented.

Most models of thermal and fluid dynamic processes in active flows assume that all the flow

elements move parallel to each other at a given station [e.g., *Baloga and Pieri, 1986; Baloga, 1987*], which results in tractable and readily solvable governing equations. However, in most lava flows, the streamlines of the fluid elements are disrupted by changes in preexisting topography, large meter-scale debris carried in the flow, the formation or disruption of levees, or internal changes in physical conditions further downstream. The disruption of streamlines by these various factors results in secondary circulations, vorticity, and perhaps local turbulence, which cause mixing of fluid elements within the flow [e.g., *Einarsson, 1949, part IV, no. 3, pp. 48-49; Booth and Self, 1973; Lipman and Banks, 1987, page 1567*]. “It’s, an assumption that the fluid hot inner core is thermally well-mixed is not entirely unrealistic, especially near the vent where velocities are highest.

A recent model of the thermal behavior of lava flows is based on a two-component approach that separates the flow into two endmember components, a hot inner core and an overriding crust [Crisp and Baloga, 1990]. This formulation permits heat to be transported between the two components, causing the crust to grow as the thermal boundary layer penetrates the interior. When disruption of the flow is strong enough to break up the crust and pull it into the core, the treatment of the core and crust as two distinct endmembers must be modified to account for exchange of mass between the two components. Cooling by entrainment has not previously been considered in theoretical models of lava flow behavior.

There is compelling evidence for the incorporation of cooler material into the hotter interior, *Lipman and Banks [1987]* and *Moore [1987]* describe abundant debris in the 1984 Mauna Loa flow ranging from semisolid to solid, which fell into the flow from levees or was created as part of the upper crust. The rubble at the base was eroded away by the lava flow in some places, and the channel was eroded from an initially strongly meandering route to a straighter path as time

proceeded [Lipman and Banks, 1987]. Videotapes of the eruption show pieces of crust and levee being pulled down into the flow where the surface is agitated and incandescent. Figures 1a and 1b demonstrate the type of lava flow behavior where evidence of entrainment is most obvious. Sudden breaks in slope (Figs. 1a-b), changes in direction or channel width, obstacles in the channel, and spillovers from levees promote the breakup of crust and can result in incandescent patches along a flow where most of the crust has been pulled into the fluid core. Sometimes, a pahoehoe to aa transition is triggered by an increase in flow rate, which causes a tube roof to collapse and allows pieces of solid roof to "become thoroughly mixed in the sluggishly moving new lava" [Peterson and Tilling, 1980]. The tendency for debris to be entrained into the core will depend on the density contrast between the debris and core as well as the intensity of mixing and agitation of the core. Some blocks will be buoyed up by the core and not sink into it.

Whether entrainment involves solidified lava, partially molten magma, or material only slightly cooler than the interior, the mixing into the core will be most effective for rapidly moving, agitated, and disrupted parts of the flow. As cooling of the interior, or other external factors, causes a slowing or cessation of flow advance, processes causing entrainment and disruption of streamlines will diminish and become less important. The degree of assimilation will depend on the size and temperature of the pieces entrained and the time spent in the core. Above and near the lava surface, an accretionary chilled coating may form on the debris, but inside the hotter inner core, partial melting and assimilation will dominate. After a flow has been emplaced, any entirely assimilated material would be impossible to recognize, but pieces of partially melted rubble that were pulled into the fluid interior have been found in Hawaiian flows, as shown in Figure 2.

in this paper, we develop a new cooling model that investigates latent heating in the core, an

exchange of mass between the crystallizing core and cooler material, and surface radiation of the exposed core. The model supplements the two-component model of *Crisp and Baloga [1990]*, in which the thermal processes affecting the core are radiative loss through cracks in the crust, continuous renewal of exposed core at the surface, and conduction from the core to the crust. The *Crisp and Baloga [1990]* model and our new model assume the core to be thermally well-mixed, in contrast to the Graetz formulation mentioned earlier. The *Crisp and Baloga [1990]* model is still valid for flows that have low rates of crystallization and entrainment. But for other flows, radiation of exposed core is a small fraction of the total heat flow budget. The new model is similar to the previous two-component model because it is only applicable to flows and parts of flows that are emplaced as a single advancing unit, such as large aa flows.

A governing equation emphasizing the effects of lava crystallization and entrainment is developed in the next section and the sensitivity of the core temperature to these mechanisms is investigated theoretically. A case study using crystallinity and emplacement data is presented for the 1984 Mauna Loa eruption to demonstrate how the model can be applied to actual flows. Finally, we discuss processes not included in the model and suggest further refinements.

A HEAT BALANCE MODEL FOR CRYSTALLINITY AND ENTRAINMENT

To formulate a mathematical model for the simultaneous processes of radiation, crystallization, and entrainment, we begin with a control volume of the core taken at a location along the flow path and identify the heat balance for this control volume. The size and character of the overriding crust are left unspecified except for the temperature, crystallinity, and material properties of the entrained material. The control volume is assumed to lose heat directly to the ambient environment by radiation through cracks and shear margins, as discussed in *Crisp and*

Baloga [1990]. Latent heat of crystallization provides a source of heat within the core, which will be examined later in more detail,

Core material could be removed from the control volume by conversion to crust, deposition in levees, or plating along the sides of a channel. Conversely, addition of volume to the core could result from the incorporation of surficial crust, solid or semisolid debris, and rubble. Entrained material is added to the control volume at a rate of Q_e ($\text{m}^3 \text{ s}^{-1}$). A volumetrically steady-state exchange is assumed so that core is removed at the same rate. For simplicity, the size of the control volume thus remains constant in this model. Relaxation of this assumption would require a separate governing equation for the evolution of the control volume, which is beyond the scope of the present investigation.

The heat balance for the core control volume is constructed from the following inventory of the relevant physical processes:

$p L A h (d\phi / dt)$	rate of heat added by crystallization
$\epsilon \sigma f T^4 A$	rate of heat lost by radiation through exposure at the surface
$p C_p T_e Q_e$	rate of heat added by entrainment
$p C_p T' Q_e$	rate of heat lost by entrainment
$p L (\Phi_e - \Phi) Q_e$	rate of heat lost by partially melting entrained material to the same crystal content as the rest of the core

The variables and parameters shown above are defined in the notation list. Each term of heat production or heat loss is considered valid at every instant while the control volume advances during its emplacement. The incorporation, remelting, and heating of the entrained material to the temperature of the core are assumed to be instantaneous.

The time rate of change of the heat content of the core is obtained by combining the

individual rate of change terms listed above. '1'bus, the rate of net heat change for the control volume of the core is given by:

$$\begin{aligned} \frac{d}{dt} (\rho C_p T A h) = & \rho L A h \frac{d\phi}{dt} - \epsilon \sigma f T^4 A \\ & + \rho C_p (T_e - T) Q_e - \rho L (\Phi_e - \Phi) Q_e \end{aligned} \quad (1)$$

Since $(\rho C_p A h)$ is constant, an alternative form for the governing equation for the core temperature is:

$$\begin{aligned} \frac{dT}{dt} = & \frac{L}{C_p} \frac{d\phi}{dt} - \frac{\epsilon \sigma f T^4}{\rho C_p h} + \frac{(T_e - T)}{\tau_e} + \frac{L (\Phi - \Phi_e)}{C_p \tau_e} \end{aligned} \quad (2)$$

TERM 1 + TERM 2 + TERM 3 + TERM 4

In deriving Equation (2), we consider all crystals nucleated during emplacement as microlites, having a volume fraction changing with time of $\phi(t)$. We also assume that the volume increase of other phenocrysts during emplacement is negligible compared to the volume increase of microlites, so we can assume that the volume fraction of phenocrysts Φ_0 is constant and the total fraction of crystals $\Phi(t)$ is the sum of Φ_0 and $\phi(t)$. To relax this assumption, $d\phi/dt$ could be replaced with $d\Phi/dt$ in Term 1 of Equation (2) to account for downstream changes in phenocryst volume. Crystallization in the flow interior releases latent heat according to the rate of change in volume fraction of microlite crystals (TERM 1). TERM 2 accounts for the radiative cooling of the core, which is partially exposed at the surface over a fractional area f . TERMS 3 and 4, respectively, model the effects of entrainment and of assimilation of cooler material into the core. In converting the form of the governing equation from (1) to (2), we introduced the parameter τ_e , defined as $A h / Q_e$, to facilitate comparison of the time scale for the entrainment process with other times of relevance, such as the crystallization time scale and emplacement duration. The

parameter τ_e is a convenient measure of the rate of exchange of material between the inner core and cooler debris, defined as the time required to completely exchange the magmatic core at a fixed location along the path of the flow. For the case of parallel-streamline flow, the exchange between cooler material and core components is absent, corresponding to an infinite value of τ_e .

The heat sink term (TERM 4) with both latent heat and τ_e accounts for the heat of fusion required to partially melt the entrained material to the same crystal abundance as the core. This last term is unimportant when the crystallinity of the entrained material is similar to that of the core. TERM 4 is always less important than TERM 3 when the difference between the temperature of the entrained material and inner core is greater than about 290°C. The ratio of TERM 4 to TERM 3 is $L(\Phi - \Phi_e) / [C_p(T_e - T)]$, so if L is 350000 J kg⁻¹ and C_p is 1200 J kg⁻¹ K⁻¹, then TERM 4 is less than TERM 3 when $[292^\circ\text{C} (\Phi - \Phi_e)] < (T_e - T)$. Thus, for values of $(\Phi_e - \Phi)$ between 0 and 1 (entrained material more crystalline than core), TERM 4 will always be less than TERM 3 when T_e is 292°C or more below T (e.g., for material cooler than about 858°C entrained in a basalt flow at 1150°C). However, for any value of T_e within about 1000°C of T , TERM 4 is of the same order of magnitude as TERM 3, and should therefore be considered in Equation (2).

THE INFLUENCE OF CRYSTALLINITY AND ENTRAINMENT ON CORE TEMPERATURE

Equation (2) provides a mathematical framework for examining the influence of crystallization and entrainment in the core of an active lava flow in comparison with cooling by radiation. To obtain mathematical solutions of (2), the crystallinity must be known explicitly as a function of time or implicitly through a temperature-crystallinity relationship.

The first approach requires knowledge of the volume fraction of microlites as a function of

time. One must either make assumptions about $\phi(t)$ (e.g., ϕ increases with time) or measure the fraction of microlites in quenched dip samples collected at different distances downstream $\phi(x)$ and use measurements of flow velocity to determine $\phi(t)$. In the second approach to using Equation (2), knowledge about the increase in fraction of crystals as a function of magma temperature is needed. This approach might be preferred if a lava is close to thermodynamic equilibrium conditions and the relationship between core temperature T and ϕ is known for the magma composition. Another way to use this approach would be to measure crystallinities of quenched downstream samples and estimate temperatures from glass composition [e.g., *Helz and Thornber, 1987*]. By replacing $d\phi/dt$ in Equation (2) with $(d\phi/dT)(dT/dt)$, the resulting equation is:

$$dT/dt = (\text{TERM2} + \text{TERM 3} + \text{TERM 4}) / [1 - (L / C_p) (d\phi / dT)] \quad (3)$$

which is identical to Equation (2), except that TERM 1 is incorporated in a new term that slows down or counteracts the rate of cooling associated with the other three terms.

At one extreme there is no exchange of mass ($Q_e = 0$) between the core and the cooler material. At the other extreme, the mass exchange could be vigorous enough to make Q_e comparable in magnitude to the net downstream flow rate. Certainly, the exchange rate could vary significantly along the paths of most real flows. For example, the 1984 Mauna Loa flow was more vigorously mixed in the channel over the first half of the flow, whereas a thick upper layer of debris and rubble and lower flow velocities were evident in the distal reaches [*Lipman and Banks, 1987*].

The steady-state entrainment rate is bounded by the two extremes identified above, that is, between zero and the downstream flow rate. For Hawaiian flows that have been observed and

documented, we consider values between approximately 1 to 25% of the downstream flow rate to be reasonable estimates for a comparative study of the influence of the entrainment process. An alternative way to view the rate of exchange between the core and the cooler debris is with the time scale τ_e . By definition, τ_e is the time required to completely exchange core with entrained material at a fixed station along the path of the flow. Hence, the limiting entrainment values (1-25%) we consider also correspond to the mass fraction of the core which has been exchanged with cooler material during emplacement.

To perform a comparative study of the influence of these processes, the functional form of the crystallization rate and its parameters must be specified. For our purposes we consider only two parameters, ϕ_{crys} and a time scale τ_{crys} , which characterize the volume percent crystallization during emplacement for a particular crystallization model. A general constraint is that total crystallinity (Φ) is less than 60% while the flow is advancing, as suggested by *Marsh* [1981].

The simplest choice of a crystallization model is a linear increase from zero at the vent to ϕ_{crys} . When $t = \tau_{\text{crys}}$, i.e., $\phi(t) = \phi_{\text{crys}} t / \tau_{\text{crys}}$. However, a more complicated dependence on time is suggested by crystallization studies of the 1984 Mauna Loa flow [*Lipman and Banks*, 1987; *Crisp et al.*, 1993]. On ascent and eruption, degassing resulted in a strongly undercooled magma. At the vent, the microlite crystallinity increased rapidly at first, in response to this disequilibrium, and then gradually approached a final value. This type of behavior could be modelled by a function such as:

$$\phi(t) = \phi_{\text{crys}} [1 - \exp(-t / \tau_{\text{crys}})] \quad (4)$$

where τ_{crys} is the time it takes the lava to reach its maximum crystallinity of ϕ_{crys} .

Figures 3a-b show the model crystallization as a function of time for different values of the parameters in Equation (4). Solutions for the core temperature using (2) and (4) appear in

Figures 4a-b. These results show the influence of crystallization in comparison with radiation from the core, for different values of the crystallization time scale and maximum crystallization. To perform this comparison we selected a nominal value of core exposure ($f = 0.01$) for Hawaiian basaltic eruptions [Crisp and Baloga, 1990]. No entrainment of cooler material is included in these examples. Even with radiation from 194 exposed core, the influence of latent heat on the core temperature is dramatic. Except for low rates of crystallization, the model shows that the heat liberated by the phase change is sufficient to raise the core temperature by tens of degrees (if the magma is erupted undercooled). Radiation rates typical of Hawaiian flows are not sufficient to counter the liberation of heat in the core for such crystallization behaviors. Note that this is a feasibility exercise (i.e., Equation (4) was chosen arbitrarily) to show that latent heat release can be significant. An undercooled magma can experience a large temperature increase due to latent heating (up to its liquidus), but this is not the case for a magma at equilibrium.

The core temperature behavior is different when entrainment is included in the model. In Figures 5 and 6, the model predictions for the core temperature are shown with different rates of entrainment τ_c and different temperatures T_c of the entrained material. The effectiveness of cooling by entrainment is strongly controlled by both parameters (Figures 5 and 6). For low rates of entrainment, latent heat can maintain a flow at or above its initial temperature if it has undergone sudden degassing and, as a result, is erupted undercooled. For flows that experience high levels of crystallization but not the strong increases in temperature after leaving the vent, either entrainment of cooler material and/or radiation from a high fraction of exposed core must be in effect to counteract the latent heat. Generally, for the type of crystallization behavior discussed in connection with Equation (4), time scales of entrainment comparable to the eruption

duration or a few multiples of it are required to offset typical radiation rates and keep core temperature from rising downstream. If entrainment rates are between 1 and 25% of the downstream flow rate, then by definition, τ_c must be 4 to 100 times larger than the emplacement duration.

Instead of using $\phi(t)$ with Equation (2), $\phi(T)$ could be used with Equation (3) to solve for core temperature. Lava lake drilling studies suggest that typical values of $d\phi/dT$ for basaltic lavas with between 0 and 60% crystals are in the range of -0.001 to -0.03 K^{-1} [e.g., *Wright and Okamura, 1977; Wright and Peck, 1978*]. For any function of ϕ that increases as T decreases, dT/dt is negative and core temperature can only decrease with time.

For the simplest case, we could assume that ϕ is a linear function of temperature. For example, if ϕ linearly increases from 0 to 0.6 over a temperature decrease from 1170°C to 1070°C , the resulting core temperature predicted by Equation (3) is shown in Figure 7 for $T_e = 700^\circ\text{C}$ and $\tau_c = 2$ and 15 days. If instead, a flow is erupted with 35% crystals at the vent, and linearly increases to 60% at 1070°C during downstream travel, then core temperature drops faster, and the maximum flow duration is cut in half (Figure 7). An intermediate example, in terms of maximum flow duration, is shown in Fig. 7 for a magma erupted with no crystals at 1140°C , which increases to 60% at 1110°C .

APPLICATION TO THE 1984 MAUNA LOA FLOW

Petrographic measurements of crystallinity can provide direct information about $\phi(t)$. Here we use temperature and crystallization constraints for the 1984 Mauna Loa lava flow to demonstrate how the model described by Equation (2) can be used to estimate the magnitude of the latent heat effect and rate of entrainment of cooler material.

The length of the 1A flow lobe of the 1984 Mauna Loa eruption may have been cooling-limited rather than eruption-rate limited [Lipman and Banks, 1987]. The temperature constraints for this flow are shown in Table 1. All the measurements are within a range of 1093 to 1155°C, and near-vent temperatures measured by thermocouple and pyrometer were consistently near 1140°C. The downstream persistence of the original microphenocrysts formed at depth and lack of crystal embayment textures indicate that the magma temperature could not have gone up much above the initial vent temperature for an extended period of time. Reliable thermocouple measurements of the hottest inner core are scarce at the distal reaches of the flow, but a temperature of 1112°C at the toe of the flow would be consistent with a thermodynamically equilibrated magma containing 60% crystals (Table 1). Temperatures lower than about 1112°C would have likely resulted in higher than 60% crystallinity and halted flow advance [Marsh, 1981].

Crystal size distribution measurements were made for quenched dip samples collected from the Mauna Loa eruption [Crisp *et al.*, 1993]. Three of these samples were collected more than a kilometer downstream, from aa breakouts that spilled over the levees. Quenched samples were not collected in the distal half of the flow (15-27 km from the vent), because of difficulty getting close to the active part of the channel and limited exposure of hotter inner core material in the distal zone. Table 2 shows the measurements of crystal abundance and size for the three downstream samples and for vent samples collected at nearly the same time. The three downstream samples inherited approximately 13-20% microphenocrysts before leaving the vent. An additional 15-25% microlites grew during emplacement before the samples were quenched. The flow should have stopped advancing after crystallizing a total of about 45% microlites ($\Phi = 60\%$ maximum possible crystallinity that allows flowage, minus an average of about 15%

preexisting microphenocrysts).

Samples collected March 30-31 indicate that the total fraction of crystals, Φ , increased from about 15% at the vent (no microlites, $\phi = 0$) to 40% (25% microlites, $\phi = 0.25$) 14 km downstream, over a period of about 4 hours [Crisp *et al.*, 1993] (Table 2, sample NER12/27). Crystal size distribution measurements of sample NER 12/27 were used to estimate crystal growth and nucleation rates averaged over those first 4 hours, using methods outlined by Marsh [1988] and Cashman and Marsh [1988]. If growth of preexisting microphenocrysts is minimal during emplacement, then the volume fraction of microlites $\phi(t)$ expected at time t for a constant growth rate G and nucleation rate J in a closed system is:

$$\phi = [1 - \exp(-k_v J G^3 t^4)] (1 - \Phi_0) \quad (5)$$

[Kirkpatrick, 1981; adjusted for the $1 - \Phi_0$ volume fraction capable of crystallizing after the microphenocrysts have formed], where k_v is a shape factor for the crystals, here assumed to be $\pi/3$ for simplicity, as for spheres. For flows in which microphenocryst growth cannot be neglected, a term could be added to Equation (5) to include the increase in microphenocryst volume. For samples taken from the upper half of the Mauna Loa flow, analysis of distributions of crystal size [Crisp *et al.*, 1993] gives estimates of $G = 3 \times 10^{-8}$ to 1×10^{-7} cm s⁻¹ and $J = 3 \times 10^4$ to 3×10^5 cm⁻³ s⁻¹ for the microlites, with lesser importance of microphenocryst growth during emplacement. Figure 8 shows a curve that connects the initial 4-hour increase calculated from Equation (5) with a smooth gradual approach to a final estimate of $\phi = 45\%$ microlites (total crystallinity $\Phi = 0.6$) after 1 day of travel. Although it took 5 days for the flow achieve its 27 km length, most parcels of lava travelled most of that length in about a day [Lipman and Banks, 1987]. A key feature of this plot is the rapid rise in crystal linity in just the first few hours of transit along the flow path. Although crystallization rates were reduced, the abundance

of crystals rose to high levels that would have eventually reached critical amounts (50-60%) and resulted in orders-of-magnitude increase in viscosity, stopping flow advance [e.g., *Marsh, 1981; Metzner, 1985*].

Figure 9 shows the core temperature predicted by Equation (2) for the case of no entrainment and the crystallization constraints for the Mauna Loa flow shown in Figure 8. *Crisp and Baloga [1990]* found that typical values of the average area fraction of exposed core (f) are between 0.001 and 0.1 for basaltic aa flows. Figure 9 shows that even for an extremely high f of 0.2, radiation alone is insufficient to counter the considerable latent heating in the early stages of the Mauna loa flow emplacement. It would have been physically possible for latent heat to raise the downstream temperature 30°C above that at the vent because the lava was erupted that much undercooked, but to conform with the temperature and crystal linity constraints, entrainment (or some other cooling mechanism) must be postulated.

We have used all four terms of Equation (2) with various combinations of parameters for the entrainment rate and temperature of the entrained material, assuming that Figure 8 shows the correct rate of crystallization. Given the rapid crystallization rate over the first few hours, no reasonable combination of constant radiation and entrainment rates is able to satisfy the temperature constraints for the Mauna Loa flow (Table 1). A reasonably good agreement with these constraints can be obtained using two sets of values to characterize the radiation and entrainment rates, one set for the near-vent regime (first 8 hours of travel) and one for the distal regime (last 16 hours). We will refer to these regimes as phases.

If the temperature of the entrained material is constant, then the predicted rate of entrainment is about 6 times higher during the first eight hours of flow compared to the last 16 hours, to balance the initially high rate of crystallization and match the final temperature estimate of about

1110-11 15°C. To meet the temperature constraints during the first phase, if the fraction of exposed core (f) is 0.1 (a rough guess based on estimates of f in *Crisp and Baloga [1990]*), then the entrainment required is 67 cm thickness of material (8 cm hr⁻¹) at a temperature of 600°C (or 46 cm at 300°C, or 121 cm at 900°C). In this model, new crust can be continually forming as core is newly exposed along cracks, shear margins, and zones of agitated flow. A portion of this crust can be entrained over and over again, along with levee debris, until the mass ratio of material entrained to core equals the ratio of entrained "thickness" to the total core thickness. We do not know the average temperature of entrained material, but the model results show the sensitivity of entrainment rate to that temperature. If f in the second phase is 0.001 (less exposed core with distance from the vent), the temperature constraints require entrainment of about 23 cm of 600°C material over the 16 hour interval (1.4 cm hr⁻¹) (or 15 cm at 300°C, or 42 cm at 900°C). Expressed in terms of mass ratios, if the entrained material was 600°C, the mass ratio of entrained material to fluid core was 15% in the first phase and 5% in the second.

A minimum thickness for an upper crust of about 22 cm after the first 8 hours (1.3 cm hr⁻¹) and an additional 15 cm over the next 16 hours (0.9 cm hr⁻¹) can be estimated from measurements and models of stationary lava lakes [e. g., *Wright and Okamura 1977, Peck et al., 1977; Shaw et al., 1977*] and pahoehoe sheet flows [*Hon et al., 1993*]. Crust can grow somewhat faster than rates predicted by pure conduction, as a result of radiative losses of the core [*Crisp and Baloga, 1990*] and convection [*Griffiths and Fink, 1992*]. In a vigorous aa flow, the crust grows even faster, due to rapid cooling of newly exposed core (e.g., continuous formation of new cracks, spallation of crustal blocks to reveal incandescent interiors, and overturning of crustal blocks). Our estimated rates of entrainment for the Mauna Loa flow suggest that these physical processes may result in crustal growth rates more than 1.5-2 times higher than rates for simple

conduction (probably at least 5 times higher, since much of the crust was not entrained). Rubble layers on the tops of lava flows are commonly thicker than what conduction alone would generate [e.g., *Moore, 1987*, Fig. 58.12]. An alternative explanation is that debris from levees and basal rubble could account for some of the discrepancy between the rate of crust growth and estimated rate of entrainment.

Generally, as velocity decreases with distance from the vent, the degree of agitation in the channel and the rate of entrainment probably also decrease. The material entrained could be the thin layer at the top surface near chilled by convection and radiation, blocks of cooler crust or levee, or a warmer crystal-rich mush beneath the solid crust. The actual values of τ_c and T_c for the Mauna Loa flow were more complicated functions of time than the step-functions we used to model the behavior in two phases. Presently, there are not enough constraints on $T(t)$, $f(t)$, and $\phi(t)$ for the Mauna Loa flow to be able to tightly constrain the possible combinations of τ_c and T_c . Instead, we have tried to show the sensitivity of the model to various plausible combinations of parameters and demonstrate how vent and downstream crystallinity measurements can be used as input to the model.

DISCUSSION

The model is applicable to lava flows consisting of a single advancing core and an overriding layer of cooler material. Compound flows formed by individual breakouts and multiple units are consistent with such a formulation, provided each breakout or lobe is treated as a single application of the model. Pahoehoe flow fields are not appropriate for this model because of the limited exposure of core at the surface, low rates of entrainment and crystallization [e.g., *Swanson, 1973; Helz et al., 1991; Hon et al., 1994*], and importance of conduction [e.g., *Hon et*

al., 1994]. The thermal histories of blocky andesite and rhyolitic flows are more appropriately modelled by considering conduction and time-temperature-crystallization relationships [Manley, 1992].

We have neglected cooling by conduction to the ground and conduction to form an upper crust, because these processes primarily affect the thickness of the core, rather than core temperature (if the core is well mixed). Although changes in thickness can affect core temperature, as shown by the h in TERM 2, our model assumes that core thickness remains constant. For long emplacement durations or thin flows, this assumption may break down and the mathematical terms for cooling by conduction should be added to this model.

Another process neglected in this model is viscous dissipation. In the Mauna Loa 1984 flow, the magnitude of viscous heating, averaged over the emplacement duration, was only 5 to 10% that of the latent heating (we have estimated viscous heating due to shearing in plane-parallel flow and not physical mixing) [Crisp *et al.*, 1993]. Viscous dissipation can be comparable in magnitude to the heat loss from the core by radiation, but this is generally not the case for basaltic flows in Hawaii and at Mt. Etna [Crisp and Baloga, 1991; Crisp *et al.*, 1993]. A term for this effect could be added to the model, if necessary, with a time dependent formulation to account for downstream changes in channel geometry and flow velocity.

Degassing is another cooling process in lava flows, which releases heat by evaporation and gas expansion. However, for most basaltic lavas, this effect is minimal. Although the volume percent vesicles in a basaltic lava can be high (60-80%), the weight percent abundances of volatiles are typically less than 0.1 % [Swanson and Fabbi, 1973; Harris and Anderson, 1983; Greenland, 1988]. In a Mauna Ulu Pahoe flow, Swanson and Fabbi [1973] documented an approximately linear decrease from about 0.05-0.07 wt% H_2O near the vent to 0.01-0.03 wt%

H₂O 12 km from the vent. In general, 1 Hawaiian summit lavas are erupted with about 0.27 wt% H₂O, 0.07 wt% S, and 0.02 wt% CO₂, and rift lavas with about 0.1 wt% H₂O, 0.015 wt% S, and <0.001 wt% CO₂ [Gerlach, 1986]. Quenched samples from a crystal-rich basaltic lava flow at Etna had a water content of 0.4 wt% at the vent, as well as 7 km downstream [Dowries, 1973]. The amount of cooling that results from degassing is a function of the weight percent volatile loss. If similar to albite and rhyolite melts, the release of 0.5 wt% H₂O from a basaltic melt should result in about 6°C cooling by adiabatic expansion and additional 7°C by evaporation [Boyd, 1961]. Most Hawaiian lavas release 0.1% or less H₂O, which would only be associated with, at most, a 3°C temperature drop. For flows with an unusually high weight fraction of dissolved volatiles, the cooling due to degassing should be considered, but the effects will be felt primarily near the vent.

Entrainment, as formulated in our model, is related to internal physical mixing in the flow. We have considered steady-state mixing between the interior of the flow and overriding crust or crystal mush zone. Material from preexisting flows and the underlying flow bed may be assimilated into an active flow, as well. At present, it is difficult to characterize the details of the entrainment process and the associated parameters. Intuitively, higher rates of entrainment should be associated with rougher terrain and more easily erodible surfaces (such as older rubbly aa flows, alluvium, and sand). Similarly, one would expect high rates of discharge or pulses in flow rate to increase the tendency for mixing of cooler layers into the interior of a flow. Low viscosity lavas with high flow velocities (high Reynolds numbers) would also tend to promote the mass exchange of entrainment. These considerations suggest fruitful areas for both theoretical and field studies of the entrainment process.

The previous two-component model of Crisp and Baloga [1990] remains applicable to flows

with limited crystallization and low rates of entrainment, which would be promoted by low flow velocities over smooth terrain and low rates of degassing-induced crystallization. However, the new model derived in this paper should be used for basaltic aa flows that undergo more than about 10% crystallization during emplacement or significant entrainment of colder material. In applying the new thermal model to lava flows, an assessment should be made on a case-by-case basis as to whether better information exists for crystallization during emplacement as a function of time (Equation (2)) or as a function of temperature (Equation (3)).

CONCLUSIONS

Crystallization and entrainment are both potentially important influences on the heat budget, dimensions, and morphology of lava flows, compared to the radiative losses from the exposed core of the flow. The model presented in this work accounts for the large amounts of heat that can be produced by crystallization during emplacement and begins to address the effects of nonplanar streamlines in the flow and mixing between the interior and cooler components. Higher rates of entrainment will favor shorter flows. The effect of higher rates of crystallization on flow length is not as simple to predict; it depends on the degree of undercooling, rates of crystallization, and total crystallinity. The latent heat of crystallization promotes slower cooling, favors longer flow lengths, but increased crystallinity levels promote an increase in bulk suspension viscosity, which favors shorter flow lengths. The effect of combined entrainment and crystallization on core temperature and maximum possible flow length can be estimated by using this model. However, further investigation is required to fully understand the influence of crystallization and entrainment on the dimensions and morphology of lava flows. The model presented in this work could be extended to predict flow length by supplementing the thermal

balance with appropriate momentum transfer equations and boundary conditions that make the flow surface and core thickness free to respond to the local dynamics of the flow.

For lava flows with more than 10% crystallization during emplacement, latent heat effects should be included in the thermal model for the interior. This source of thermal energy may be balanced by an exchange of mass between the core of the flow and its surroundings. Although we have modeled this exchange as a steady-state process, it is clear from the application of the model to the Mama Loa flow, that entrainment must be a time-dependent process like surface renewal and core exposure as discussed in *Crisp and Baloga* [1990].

This study has demonstrated that measurements of crystallinity along the path of a flow are critical for understanding the heat budget while the flow is active. At present, such crystallization data are extremely limited. Processes associated with the disruption of flow lines in the interior of an active flow and mass exchange, with cooler elements, such as the crust, are important for understanding the heat budget. Field or theoretical methods for characterizing entrainment or mass exchange mechanisms are also needed to advance our understanding of thermal processes in lava flows and their relation to flow dimensions and morphologies.

NOTATION

A	= planimetric area of the upper surface of the control volume (Ah) of the core
C_p	= heat capacity of lava in the core
ϵ	= emissivity of lava in the core
f	= area fraction of exposed core at surface
G	= crystal growth rate (cm s^{-1})
h	= average core thickness

J	=	crystal nucleation rate ($\text{cm}^{-3} \text{ s}^{-1}$)
k_v	=	crystal shape factor = average crystal volume divided by four times the average crystal radius cubed
L	=	average latent heat (J kg^{-1})
Φ	=	total volume fraction of crystals in the core = $\phi + \Phi_o$
Φ_e	=	total volume fraction of crystals in the entrained material
Φ_o	=	volume fraction of phenocrysts at the vent
ϕ	=	volume fraction of microlites formed in the core during emplacement
ϕ_{crys}	=	maximum volume fraction of microlites attained during emplacement
Q_e	=	volume rate of entrainment of cooler material into core
ρ	=	density of lava in the core
σ	=	Stefan-Boltzmann constant
T	=	core temperature (Kelvin, in Equations (1-3))
T_e	=	temperature of entrained material (Kelvin, in Equations (1-3))
τ_e	=	entrainment time scale
τ_{crys}	=	crystallization time scale (time to achieve maximum microlite crystallinity)
τ	=	lava flow emplacement duration
t	=	time since beginning of emplacement
x	=	distance

Acknowledgments. This work was carried out at the Jet Impulsion Laboratory, California Institute of Technology, under a contract with the National Aeronautics and Space Administration. We thank C. Kilburn and S. Anderson for thorough reviews and T. Neal, J. I. Griggs, and S. Finnemore for providing photos,

REFERENCES

- Baloga, S., lava flows as kinematic waves, *J.Geophys.Res.*, 92, 9271-9279, 1987.
- Baloga, S., and D.Pieri, Time-dependent profiles of lava flows, *J.Geophys.Res.*, 91, 9543-9552, 1986.
- Booth, B., and S. Self, Rheological features of the 1971 Mount Etna lavas, *Phil. Trans. R. Soc. Lond. A*, 274, 99-106, 1973.
- Boyd, F.R., Welded tuffs and flows in the rhyolite plateau of Yellowstone Park, Wyoming, *Geol. Soc. Am. Bull.*, 72, 387-426, 1961.
- Cashman, K. V., and B.D. Marsh, Crystal size distribution (CSID) in rocks and the kinetics and dynamics of crystallization I. Makaopuhi lava lake, *Contrib. Mineral. Petrol.*, 99, 292-305, 1988.
- Crisp, J., and S. Baloga, A model for lava flows with two thermal components, *J.Geophys.Res.*, 95, 12,555-12,570, 1990.
- Crisp, J. A., and S.M.Baloga, Thermal processes in lava flows (abstract), *Lunar Planet. Sci. Conf. 22nd*, pp.257-258, 1991.
- Crisp, J., K.V. Cashman, J.A. Bonini, S.B. Houghton, and D.C. Pieri, Crystallization history of the 1984 Mauna Loa lava flow, submitted to *J. Geophys. Res.*, 1993.
- Downes, M. J., Some experimental studies on the 1971 lavas from Etna, *Phil. Trans. R. Soc. Lond. A*, 274, 55-62, 1973.
- Einarsson, 'P.', The flowing lava. Studies of its main physical and chemical properties, in *The eruption of Hekla 1947-1948*, edited by T. Einarsson, G. Kjartansson, and S. Thorarinsson, Visindafelg Islendinga, Reykjavik, Iceland, 1949.
- Emerson, O.H., The formation of aa and pahoehoe, *Am. J. Sci.*, 12, 109-114, 1926.
- Gerlach, 'P'. M., Exsolution of H₂O, CO₂, and S during eruptive episodes at Kilauea Volcano, Hawaii, *J. Geophys. Res.*, 92, 12177-12185, 1986.
- Ghiorso, M. S., Chemical mass transfer in magmatic processes, 1. Thermodynamic relations and numerical algorithms, *Contrib. Mineral. Petrol.*, 90, 107-120, 1985.

- Ghiorso, M. S., and I.S.E. Carmichael, Chemical mass transfer in magmatic processes, 11. Applications in equilibrium crystallization, fractionation and assimilation, *Contrib. Mineral. Petrol.*, 90, 121-141, 1985.
- Greenland, L.L., Gases from the 1983-84 East-rift eruption, in The Puu Oo eruption of Kilauea Volcano, Hawaii: Episodes 1 through 20, January 3, 1983, through June 8, 1984, edited by E.W. Wolfe, U.S. Geological Survey, Prof. Pap., 1463, 145-153, 1988.
- Griffith, R. W., and J.H. Fink, The morphology of lava flows in planetary environments: predictions from analog experiments, *J. Geophys. Res.*, 97, 19739-19748, 1992.
- Guest, J.E., C.R.J. Kilburn, H. Pinkerton, and A.M. Duncan, The evolution of lava flow-fields: observations of the 1981 and 1983 eruptions of Mount Etna, Sicily, *Bull. Volcanol.*, 49, 527-540, 1987.
- Harris, D. M., and A. I. Anderson, Jr., Concentrations, sources, and losses of H_2O , CO_2 , and S in Kilauea basalt, *Geochim. Cosmochim. Acta*, 47, 1139-1150, 1983.
- Harrison, C.G.A., and C. Rooth, The dynamics of flowing lavas, in *Volcanoes and Tectonosphere*, edited by H. Aoki and S. Iizuka, pp. 103-113, University of Tokyo, Tokyo, 1976.
- Helz, R.T., and C.R. Thornber, Geothermometry of Kilauea Iki lava lake, Hawaii, *Bull. Volcanol.*, 49, 651-668, 1987.
- Helz, R.T., M. Mangan, K. Hon, and L. Simmons, Thermal history of the current Kilauean East Rift eruption, *EOS Trans. AGU*, 557-558, 1991.
- Hon, K., J. Kauahikaua, R. Denlinger, and K. McKay, Emplacement and inflation of pahoehoe sheet flows -- Observations and measurements of active Hawaiian lava flows, *Geol. Soc. Am. Bull.*, in press, 1994.
- Hulme, G., and G. Fielder, Effusion rates and rheology of lunar lavas, *Proc. Roy. Soc. London, Ser. A*, 285, 227-234, 1977.
- Jaggard, I. A., Distinction between pahoehoe and aa or block lava, *Volcano Letter*, 281, 1-3, 1930.
- Kilburn, C.R.J. and R.M.C. Lopes, General patterns of flow field growth: Aa and blocky lavas, *J. Geophys. Res.*, 96, 19721-19732, 1991.
- Kirkpatrick, R. J., Kinetics of crystallization of igneous rocks, *Reviews in Mineralogy*, 8, 321-398, 1981.

- Kouchi, A., A. Tsuchiyama, and I. Sunagawa, Effect of stirring on crystallization kinetics of basalt: texture and element partitioning, *Contrib. Mineral. Petrol.*, 93, 429-438, 1986.
- Lipman, P. W., and N.G. Banks, Aa flow dynamics, Mauna Loa 1984, U.S. *Geol. Surv. Prof. Pap.*, 1350, 1527-1567, 1987.
- Macdonald, G. A., Pahoehoe, aa, and block lava, *Am. J. Sci.*, 251, 169-191, 1953.
- Manley, CR., Extended cooling and viscous flow of large, hot rhyolite lavas: implications of numerical modeling results, *J. Volcanol. Geotherm. Res.*, 53, 27-46, 1992.
- Marsh, B.D., On the crystallinity, probability of occurrence, and rheology of lava and magma, *Contrib. Mineral. Petrol.*, 78, 85-98, 1981.
- Marsh, B. D., Crystal size distribution (CSD) in rocks and the kinetics and dynamics of crystallization 1. Theory, *Contrib. Mineral. Petrol.*, 99, 277-291, 1988.
- Metzner, A.B., Rheology of suspensions in polymeric liquids, *J. Rheol.*, 29, 739-775, 1985.
- Moore, H. J., Preliminary estimates of the rheological properties of the 1984 Mauna Loa lava, U.S. *Geol. Survey Prof. Paper 1350*, pp. 1509-1588, 1987.
- Peck, D.L., M.S. Hamilton, and H.R. Shaw, Numerical analysis of lava lake cooling models: Part 11, Application to Alac lava lake, Hawaii, *Am. J. Sci.*, 277, 415-437, 1977.
- Peterson, D. W., and R.J. Tilling, Transition of basaltic lava from pahoehoe to aa, Kilauea volcano, Hawaii: Field observations and key factors, *J. Volcanol. Geotherm. Res.*, 7, 271-293, 1980.
- Pinkerton, H., and R.S.J. Sparks, The 1975 sub-terminal lavas, Mount Etna: A case history of the formation of a compound lava field, *J. Volcanol. Geotherm. Res.*, 1, 167-182, 1976.
- Pinkerton, H., and R.J. Stevenson, Methods of determining the rheological properties of magmas at sub-liquidus temperatures, *J. Volcanol. Geotherm. Res.*, 5, 47-66, 1992.
- Ryerson, F.J., H.C. Weed, and A.J. Piwinski, Rheology of subliquidus magmas 1. Picritic compositions, *J. Geophys. Res.*, 93, 3421-3436, 1988.

- Scittle, M., Lava rheology: Thermal buffering produced by the latent heat of crystallization (abstract), *Lunar Planet. Sci. Conf. 10th*, pp. 1107-1109, 1979.
- Shaw, H.R., M.S. Hamilton, and D.L. Peck, Numerical analysis of lava lake cooling models; Part 1, Description of the model, *Am. J. Sci.*, 277, 384-414, 1977.
- Sparks, R. S. J., and 11, Pinkerton, Effect of degassing on rheology of basaltic lava, *Nature*, 276, 385-386, 1978.
- Stasiuk, M. V., C. Jaupart, and R.S.J. Sparks, Influence of cooling on lava-flow dynamics, *Geology*, 21, 335-338, 1993.
- Swanson, D.A., and B.P. Fabbri, Loss of volatiles during fountaining and flowage of basaltic lava at Kilauea volcano, Hawaii, *J. Res. U.S. Geol. Survey*, 1, 649-658, 1973.
- Wadge, G., Effusion rate and the shape of aa lava flow-fields on Mount Etna, *Geology*, 6, 503-506, 1978.
- Wilson, L., and E.A. Parfitt, The formation of perched lava ponds on basaltic volcanoes: the influence of flow geometry on cooling-limited lava flow lengths, *J. Volcanol. Geotherm. Res.*, 56, 113-123, 1993.
- Wright, T.L., and R.T. Okamura, Cooling and crystallization of tholeiitic basalt, 1965 Makaopuhi lava lake, Hawaii, *U.S. Geol. Survey Prof. Pap.*, 1004, 78pp., 1977.
- Wright, T.L., and D.L. Peck, Crystallization and differentiation of the Alac magma, Alac lava lake, Hawaii, *U.S. Geol. Surv. Prof. Pap.*, 935-C, 20pp., 1978.

S. Baloga, Proxemy Research, Inc., 2052.8 Faircroft Lane, Laytonville, MD 20882, J. Crisp, MS 83-S01, Jet Propulsion Laboratory, 4800 Oak Grove Drive, Pasadena, CA 91109

FIGURE CAPTIONS

Fig. 1a. Entrainment of crust due to sudden break in slope in the 1984 Mauna Loa lava flow. Just past the change in slope, the lava is incandescent at the surface. Photo by J.D. Griggs, U.S. Geological Survey.

Fig. 1b. Photo by J.D. Griggs, U.S. Geological Survey.

Fig. 2. piece of basalt rubble (outlined in chalk) entrained in a basaltic flow and partially melted by the host lava. Photo by S. Finnemore, University of Hawaii.

Fig. 3a. Volume fraction of microlites formed during emplacement as a function of time, according to the “generic” model of crystallization in Equation (4). Examples are shown for $\phi_{\text{crys}} = 0.5$ and different values of the crystallization time scale τ_{crys} (in clays).

Fig. 3b. Same as in Fig. 3a, for $\tau_{\text{crys}} = 2$ clays and different values of ϕ_{crys} .

Fig. 4a. Core temperature as a function of time, derived from Equation (1), with no entrainment (Terms 3 and 4 equal to zero), for different rates of crystallization (τ_{crys} in clays) shown in Figure 3a, an average fraction of exposed core of $f = 0.01$, $\phi_{\text{crys}} = 0.6$, and initial temperature of 1140°C .

Fig. 4b. Same as in Fig. 4a, for $\tau_{\text{crys}} = 2$ days and different values of ϕ_{crys} .

Fig. 5. Core temperature as a function of time, derived from Equations (2) and (4), with $\phi_{\text{crys}} = 0.6$, $\tau_{\text{crys}} = 2$ days, initial temperature of 1140°C , $h = 5$ m, $f = 0.005$, $T_e = 300^\circ\text{C}$, and four different rates of entrainment (τ_e shown in days). The case of no entrainment is shown by the curve for $\tau_e = 00$.

Fig. 6. Core temperature as a function of time, derived from Equations (2) and (4), with $\phi_{\text{crys}} = 0.6$, $\tau_{\text{crys}} = 2$ days, initial temperature of 1140°C , $h = 5$ m, $f = 0.005$, and $\tau_e = 20$ days, shown for three different temperatures of entrained material T_e .

Fig. 7. Solid curves show core temperature predicted by Equation (3), for a low entrainment rate ($\tau_e = 15$ days) and dashed curves are for a high entrainment rate ($\tau_e = 2$ days). The top pair of curves are for an initial temperature of 1170°C with no crystals, linearly increasing to 60% crystals at 1070°C ($\phi = 8.658 - 0.0067T$, T in Kelvin). The middle set of curves are for a magma with no crystals at the vent erupted at 1140°C , increasing to 60% crystals at 1110°C ($\phi = 28.260 - 0.020T$). The lowest set of curves are for a 1130°C magma with 35% phenocrysts at the vent, increasing to 60% crystals at 1070°C ($\phi = 5.846 - 0.004167T$).

Fig. 8. Estimate of the rate of crystallization during flow advance for the 1984 Mauna Loa flow. See text for discussion.

Fig. 9. Results of the model of Equation (1) for the Mauna Loa flow with radiative cooling and latent heating (no entrainment). Average fraction of exposed core of $f = 0.005$ or 0.2 . Crystallization rate as shown in Figure 8.

TABLE 1. Temperature Constraints for the 1984 Mauna Loa Flow

km from vent	1' ("c)		
	Field Measurements ^a	Thermodynamic Equilibrium ^b	Glass Geothermometry ^c CaO, MgO
0-0.1	1140 ± 5		1140-1155**
(0-0.1)			1137-48, 125-148***
10-12	135 ± 5		
14.2	126	1130	1112-24, 093-113
16.5	> 1125'		
20.4	> 1103"		
24.5	> 1086'		
27		1112-1130	

^a Thermocouple and pyrometer measurements in *Lipman and Banks* [1987] and unpublished data provided by J. Lockwood, U.S. Geological Survey, Hawaiian Volcano Observatory.

^b Prediction of equilibrium temperature for the Mauna Loa magma at 1 atm, water-free, using the model of *Ghiorso* [1985] and *Ghiorso and Carmichael* [1985] (*Crisp et al.*, [1993]), if total crystallinity 14 km from the vent is 0.39, as found in the downstream quench sample N18R12/27 [*Crisp et al.*, 1993], or between 0.39 and 0.6 at the toe of the flow (*Marsh* [1981] suggests 0.6 is an upper bound for the crystallinity of flowing lava).

^c Range of temperatures (including analytical uncertainty) predicted using the *Helz and Thornber* [1987] geothermometers for CaO and MgO content of Kilauea Iki lava lake [*Crisp et al.*, 1993]. Where two ranges are separated by commas, the first is the temperature from CaO content, the second is from MgO.

'thermocouple failed before equilibrium was reached.

** first 10 hours of the eruption.

*** first 50-300 hours of the eruption,

TABLE 2. Crystal Abundances in Near-Vent and Far-Vent Quenched Samples^a of the 1984 Mama Loa Flow

Date	Distance from vent (km)	Travel time (minutes)	Sample	Total % Crystals	Volume % Microphenocrysts	Volume % Microlites
3/31	0		NER12/28	21.8	19.6	2.2
3/30	14	230	NER12/27	39.0	13.7	25.3
4/6	0		NER12/46	3.2	13.2	0
4/6	11	110	NER12/48	24.1	9.0	15.1
4/8	0		NER 12/56	16.9	15.4	1.5
4/8	6	100	NER 12/57	22.3	9.0	13.3

^a Samples and sample descriptions provided by J. Lockwood, U.S. Geological Survey, Hawaiian Volcano Observatory, and described in *Crisp et al. [1993]*. Travel time is estimated to be roughly 2 times the surface flow velocity, measured at similar times and locations, from data in *Lipman and Banks [1987]*.

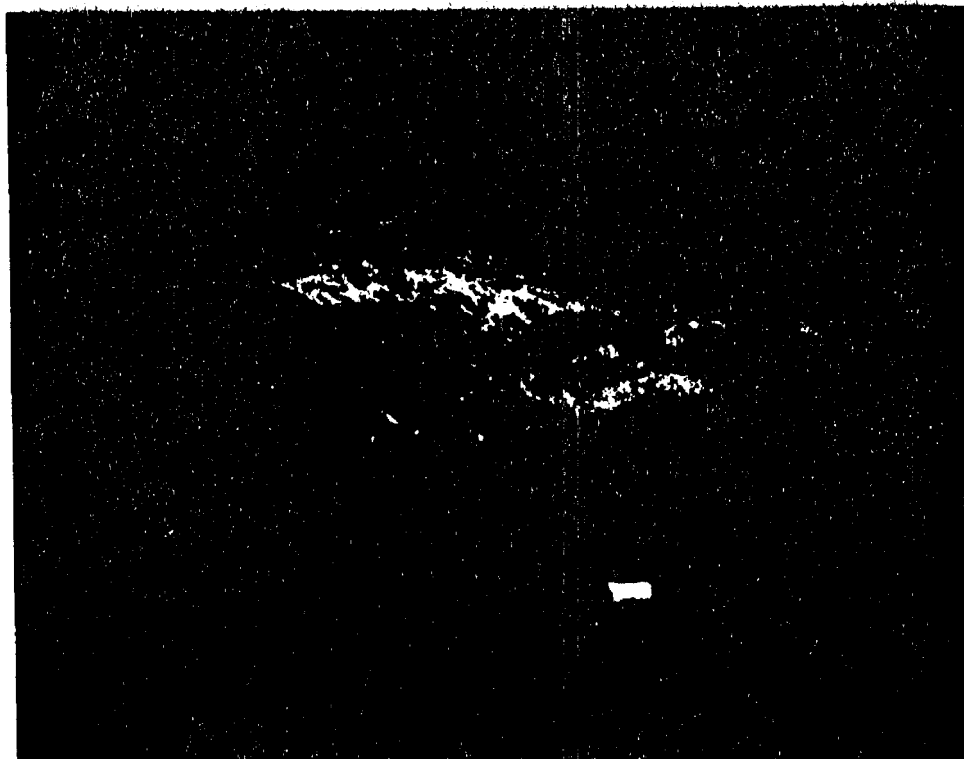


Fig. 1a

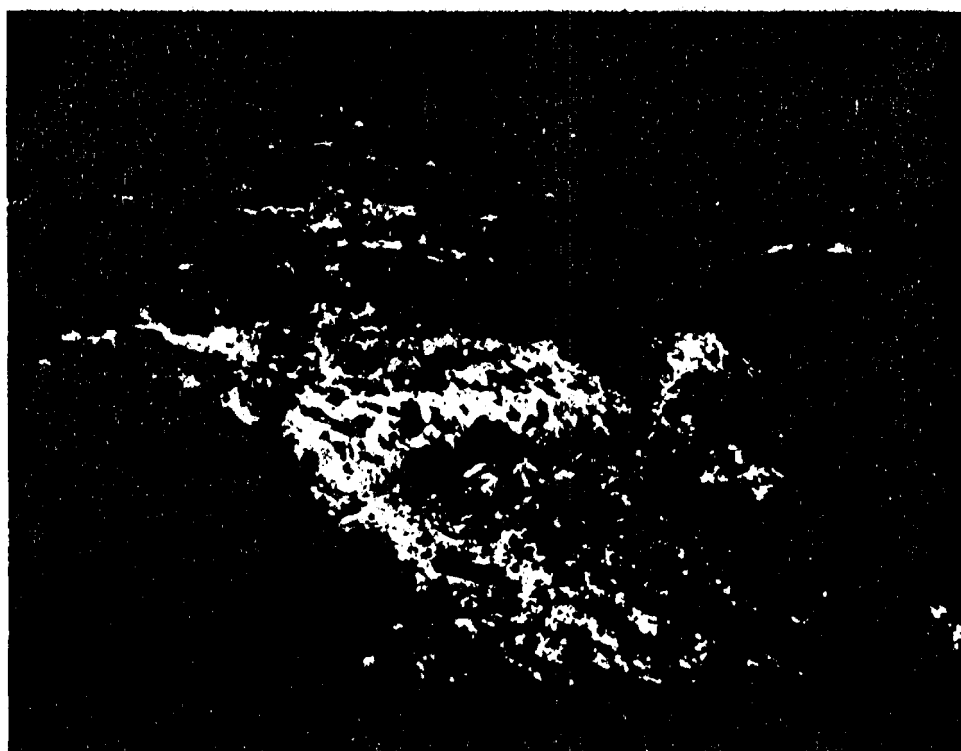
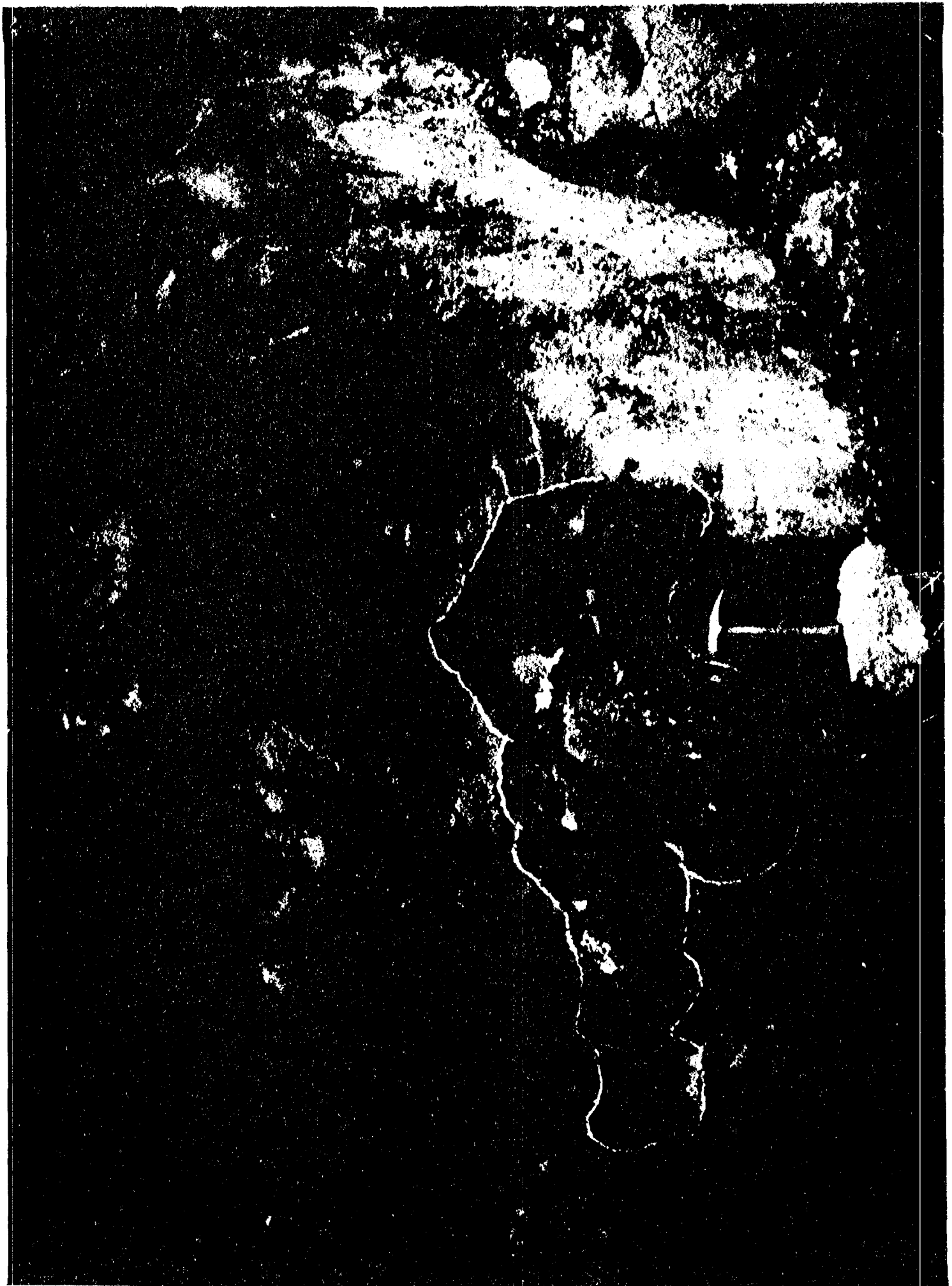


Fig. 1b



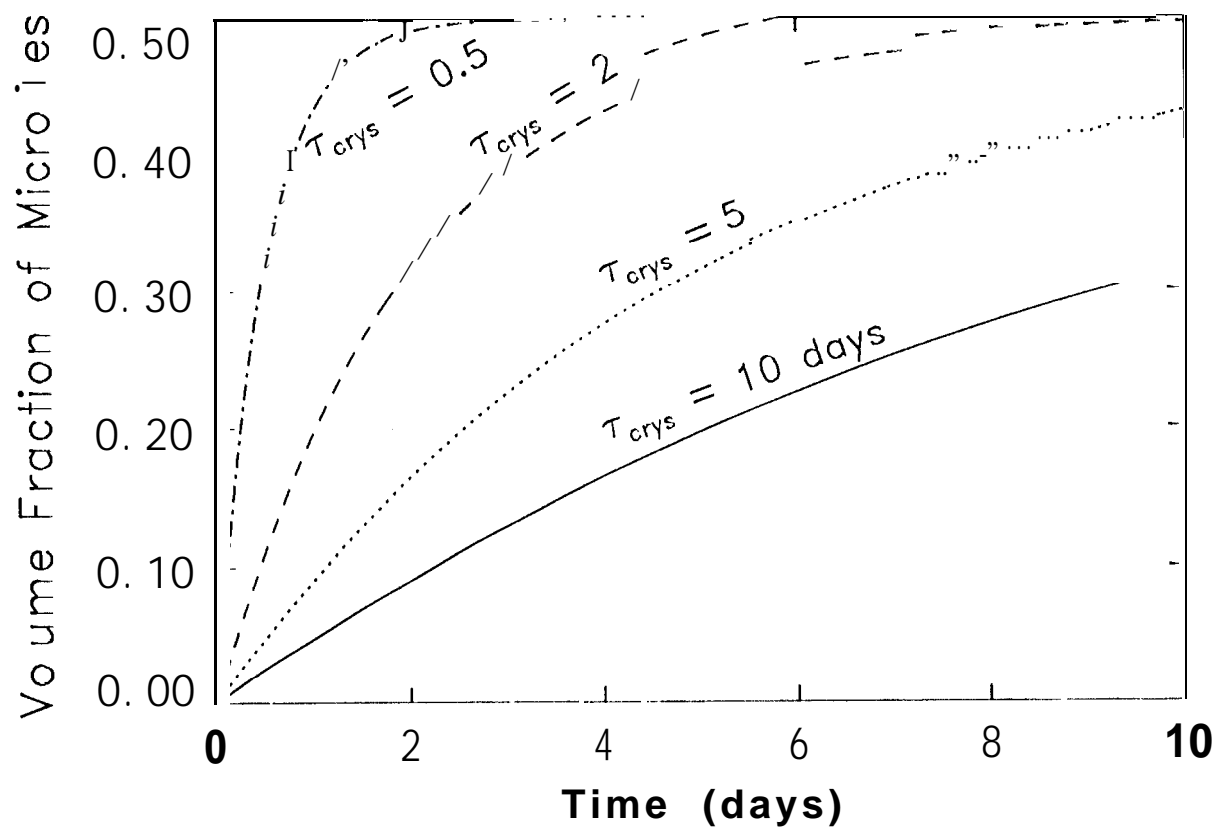


Fig. 3a

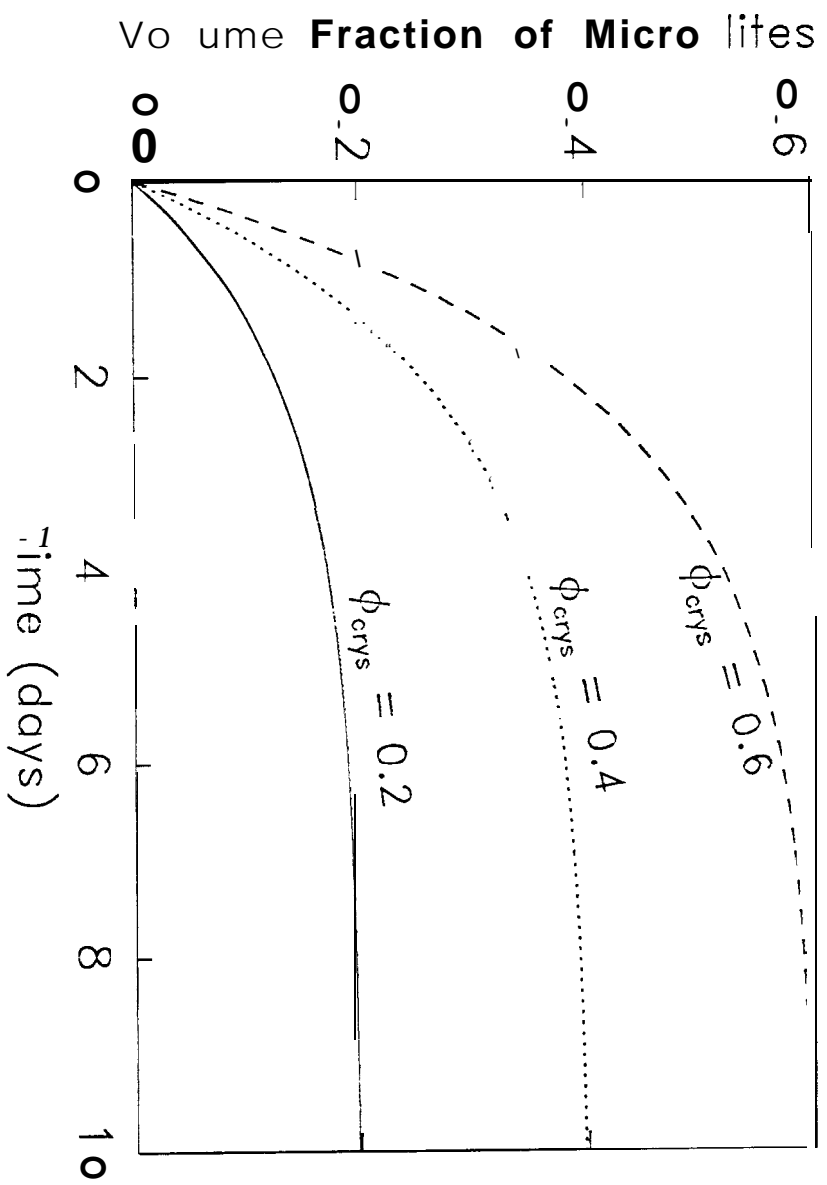


Fig. 3b

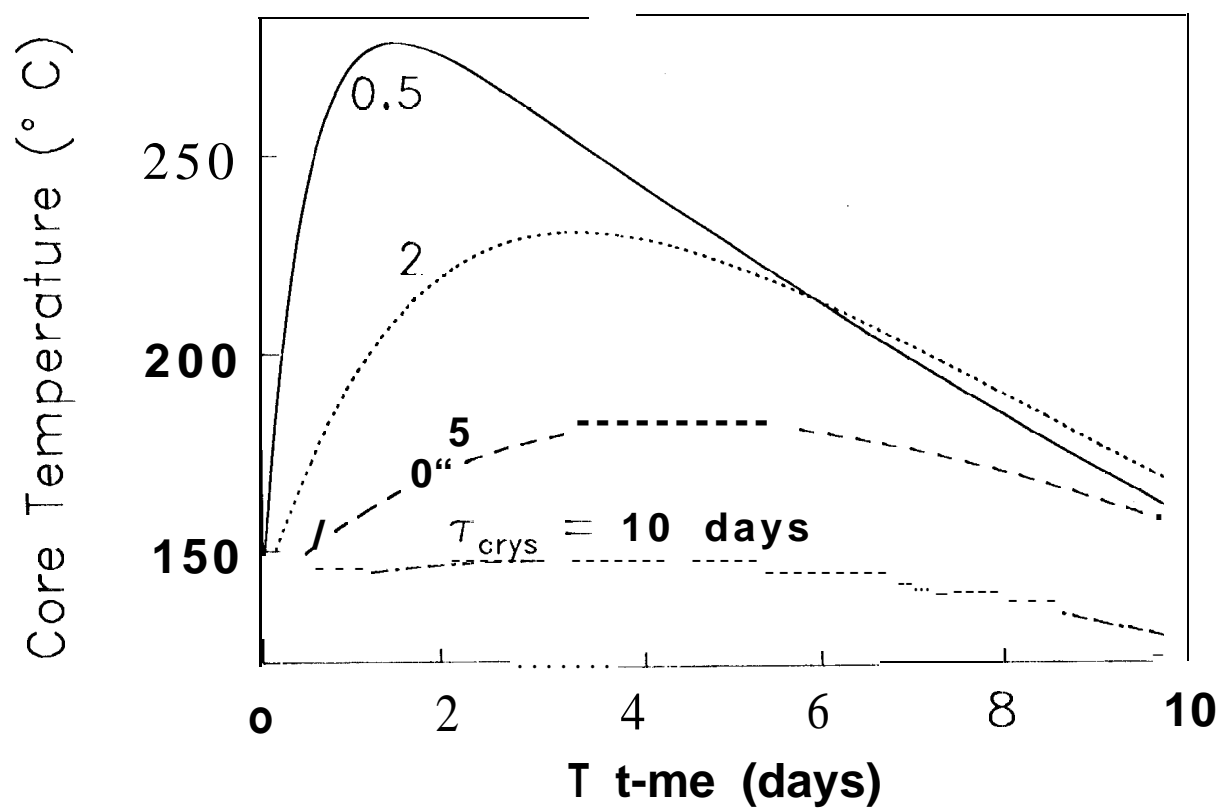


Fig. 4a

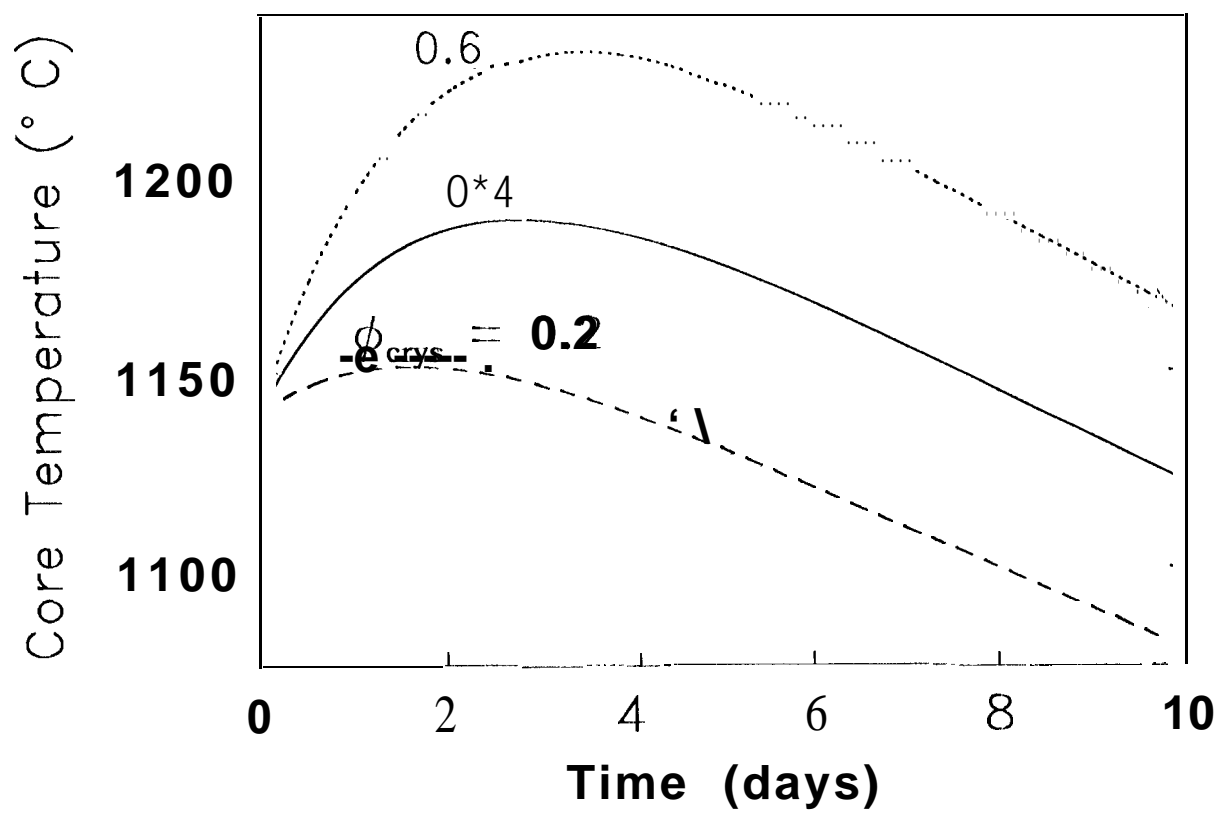


Fig.4b

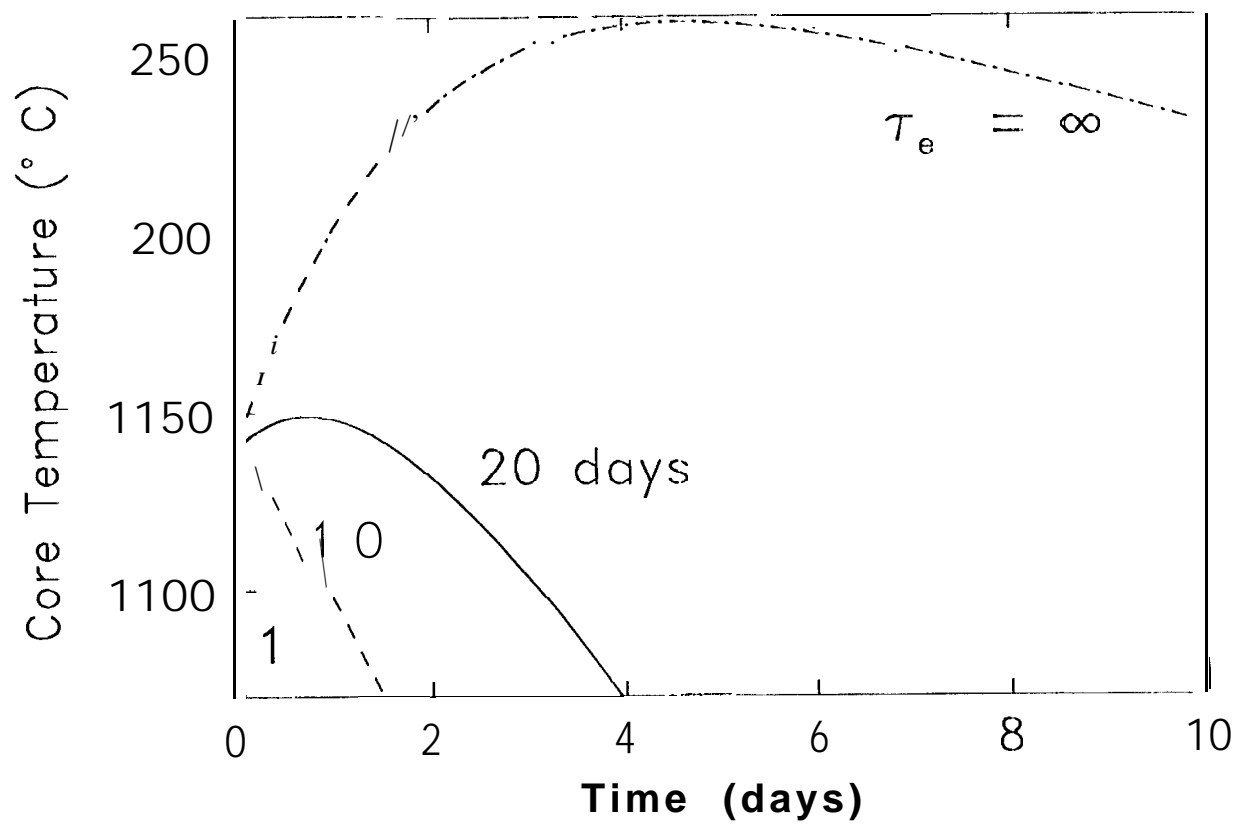


Fig S

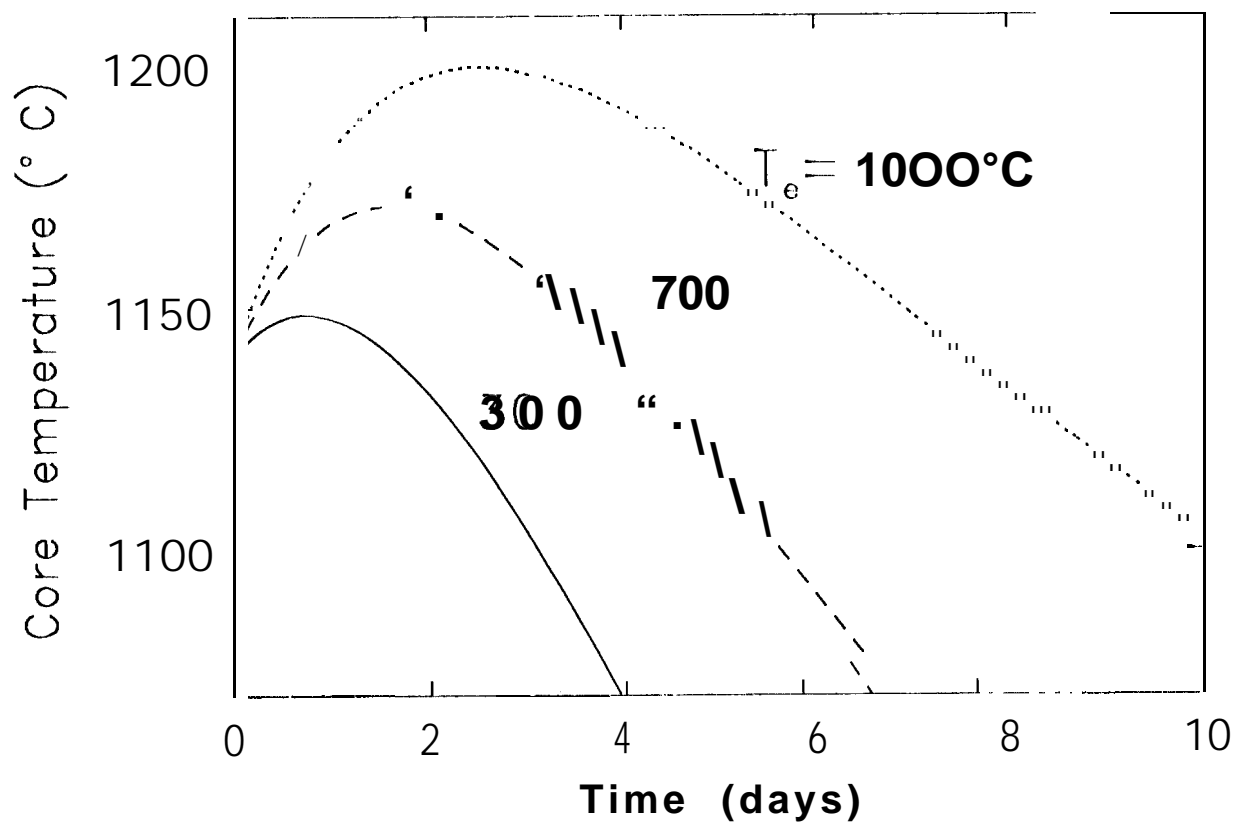


Fig. 6

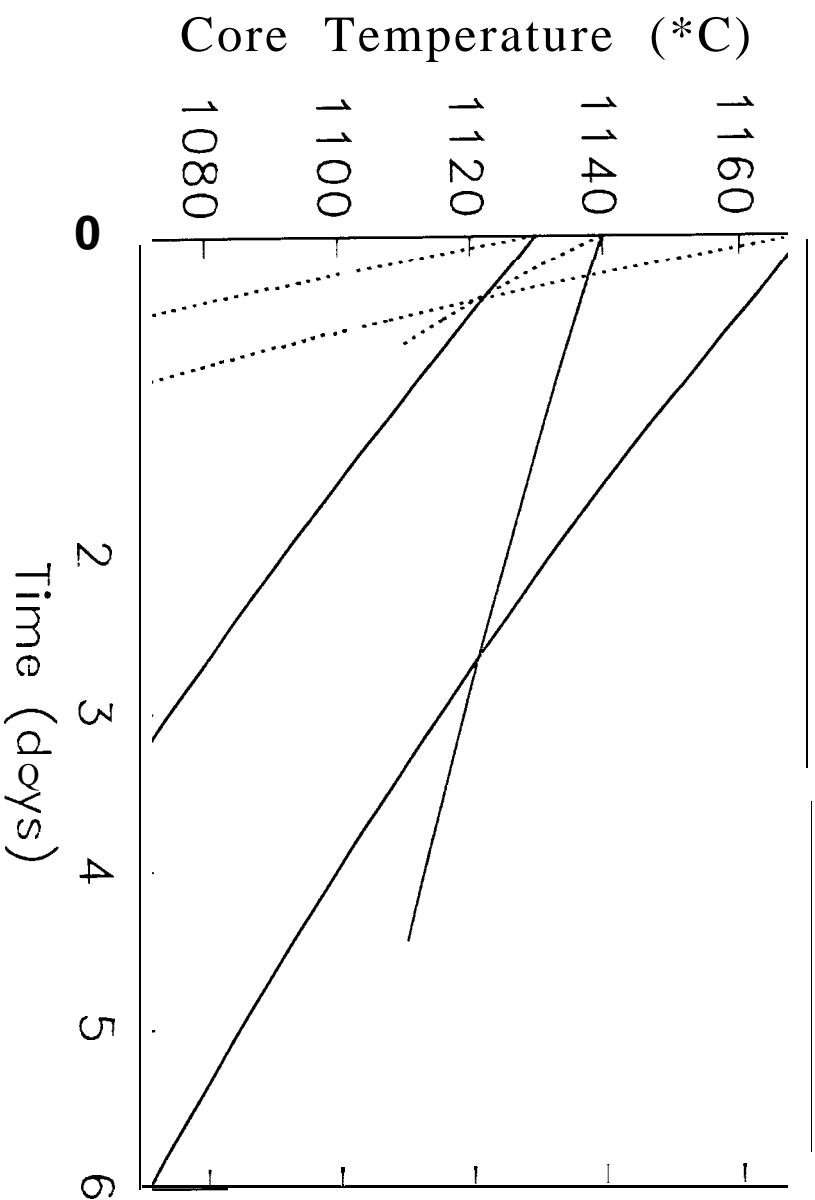


Fig. 7

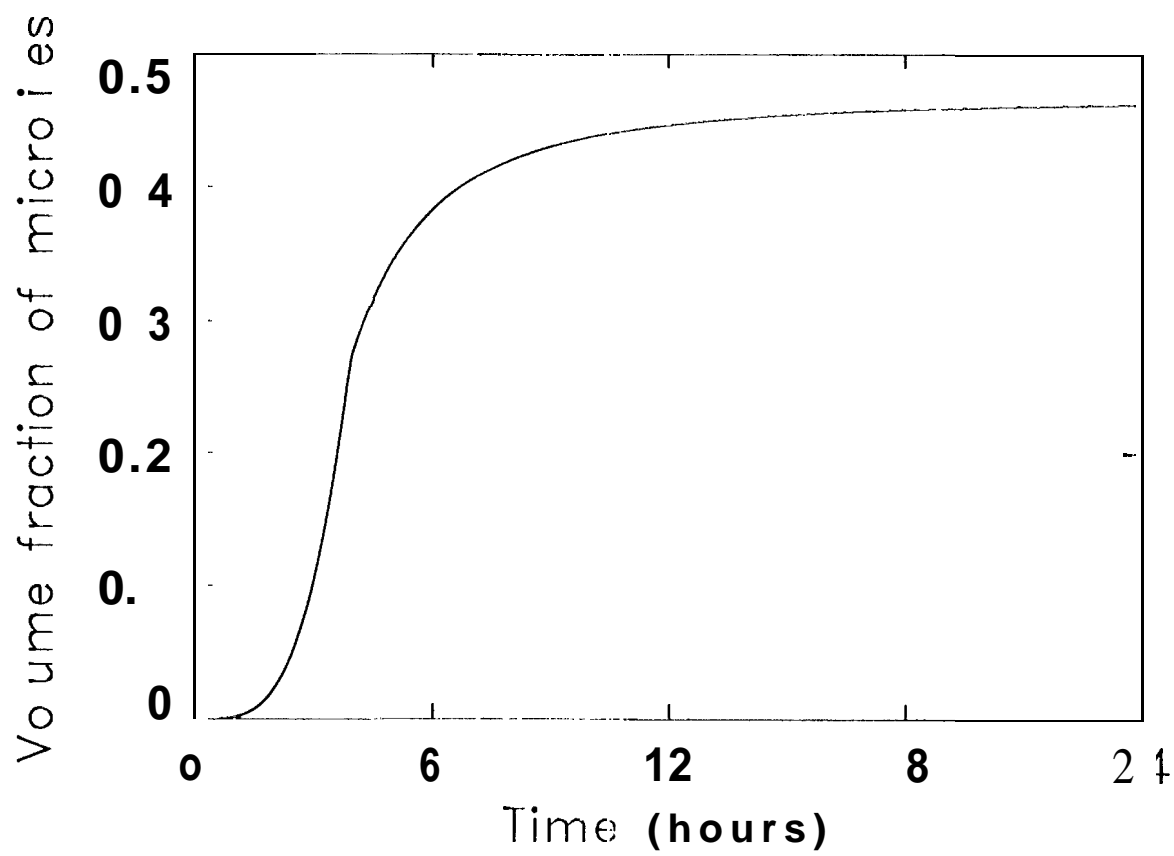


Fig. 8

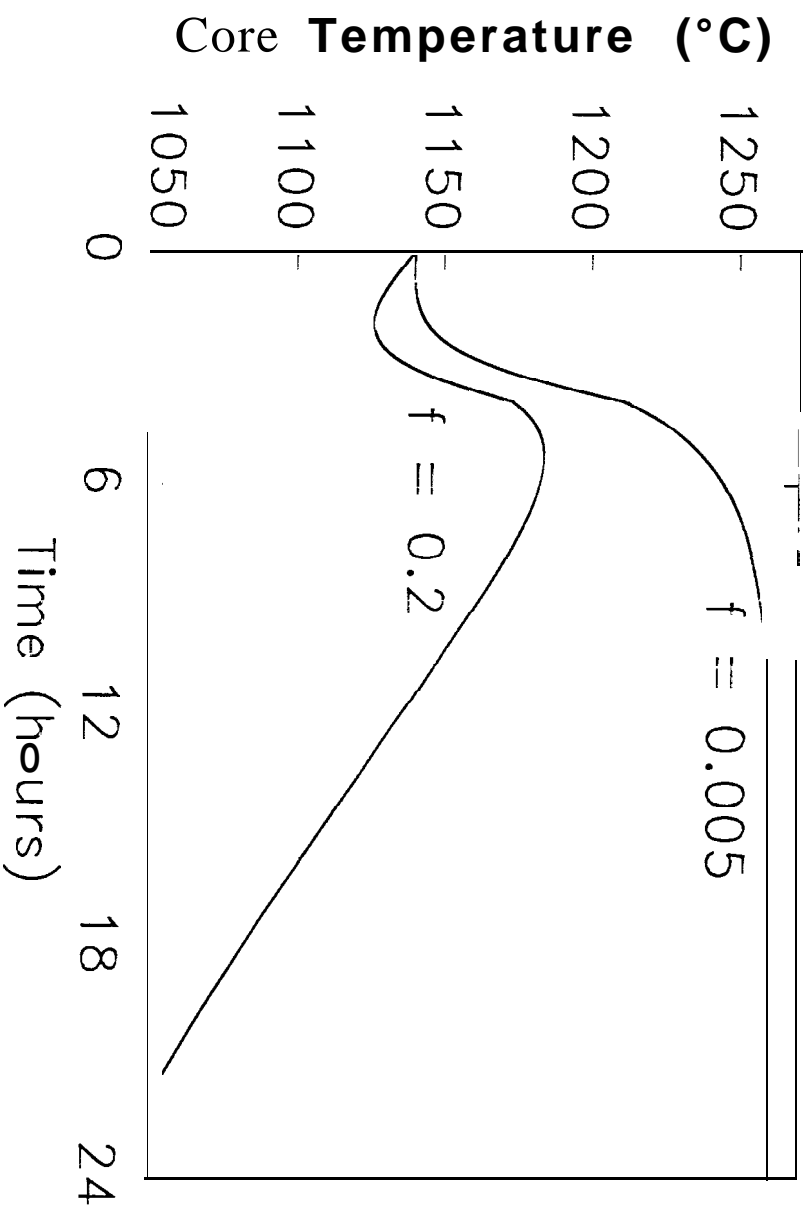


Fig. 9